Available online at www.sciencedirect.com
ScienceDirect
Ceramics International 36 (2010) 1857–1861
CERAMICS INTERNATIONAL
www.elsevier.com/locate/ceramint

Optical, thermal and dielectric properties of $Bi_4(TiO_4)_3$ ceramic powders

G. Bhaskar Kumar, S. Buddhudu *

Department of Physics, Sri Venkateswara University, Tirupati 517502, India

Received 4 January 2010; received in revised form 8 February 2010; accepted 17 March 2010
Available online 28 April 2010

Abstract

Bismuth titanate ($Bi_4(TiO_4)_3$) ceramic powders have been synthesized by using a solid state reaction method. Prominently intense *blue* emission at 480 nm has been measured with an excitation at 418 nm. The reason for the observance of such a blue emission from this ceramic powder has been explained. The phase formation has been investigated by X-ray diffraction analysis (XRD). The morphology and composition of the ceramic powders have been studied from the measurement of SEM and EDS profiles. FTIR and Raman spectra have also been recorded to analyze the presence of functional groups and Raman active modes in the $Bi_4(TiO_4)_3$ ceramic powders. The sintering temperature has been optimized to be 1100 °C based on the measured TG–DTA profiles of the as prepared material. Besides these, dielectric properties of ceramic powder in the frequency range of 200 Hz–3 MHz at 300 K have also been carried out.

Keywords: A. Powders: solid state reaction; B. Spectroscopy; Titanates

1. Introduction

Over the past few years, a great deal of research activities have been made on lead based and lead free ferroelectric materials because of their potential applications in different kinds of devices like storage information and photonic devices, piezoelectric actuators and infrared sensors etc. Among them, Bismuth titanate has potential applications in memory storage, optical display and other electro-optical devices due to its unique ferroelectric, piezoelectric, and electro-optic switching behaviors [1–5].

Oxide-based inorganic ceramic phosphors have been investigated for their optical applications like high-resolution devices such as cathode-ray tubes, electroluminescent devices, plasma display panels and field emission displays [6,7]. Luminescence of the titanate-type compounds could be found immensely useful in optoelectronic applications. TiO_2 possess good mechanical resistance and stability, and therefore it has widely been used in the development of certain stable host matrices like $BaTiO_3$, $SrTiO_3$, $CaTiO_3$ and a few TiO_2-based oxide composites like TiO_2–SiO_2, TiO_2–CeO_2, TiO_2–ZrO_2 and TiO_2–Fe_2O_3 [8–10]. $BaTiO_3$ and $SrTiO_3$, are two known examples, which attract a renewed interest due to their efficient luminescence performance from perovskite structured materials [11]. Upon realizing the existing importance of bismuth titanate, we have prepared stable $Bi_4(TiO_4)_3$ ceramic powders by a conventional solid state reaction method and thus report here the results concerning optical, thermal and dielectric properties of this material.

2. Experimental details

Bismuth titanate ($Bi_4(TiO_4)_3$) ceramic powders were synthesized by using a solid state reaction method. High pure and analytical reagent grade chemicals such as Bi_2O_3 and TiO_2 were used as the starting materials. Those chemicals were weighed based on the calculated composition and it was finely powdered using mortar and a pestle for 2 h to obtain homogeneous precursor. The mixture was then put into a silica crucible and heated from the room temperature to 1100 °C and it was kept at the same temperature for 5 h in an electrical tubular furnace.

The structure of the prepared ceramic powder was characterized on a XRD 3003 TT Seifert diffractometer with Cu Kα radiation (λ = 1.5406 Å) at 40 kV and 20 mA and the 2θ range was varied between 20° and 80°. The morphology of the ceramic powder was observed on a Zeiss EVO MA 15 Scanning Electron Microscope. The elemental analysis of the synthesized

* Corresponding author. Tel.: +91 877 2261611; fax: +91 877 2249273.
E-mail address: profsb_svuniv@hotmail.com (S. Buddhudu).

0272-8842/$36.00
doi:10.1016/j.ceramint.2010.03.023

products was carried out using the Oxford EDAX equipment (INCA-Penta Fet X3) attached to the SEM system. FTIR spectrum of the sample was recorded on a Nicolet IR-200 spectrometer using KBr pellet technique from 4000 cm^{-1} to 400 cm^{-1}. Raman spectrum was recorded by using a high-resolution Jobin Yvon Model HR800UV system attached with a He–Ne laser (633 nm) as the excitation source having an output power of 15 mW with a laser beam spot size of 100 μm using appropriate lens system. The photoluminescence spectrum of this powder was recorded on a Jobin Yvon Fluorolog-3 Fluorimeter with a Xe-arc lamp (450 W) as an excitation source. Thermogravimetry (TG) and differential thermal analysis (DTA) were performed for the precursor in N_2 atmosphere at a heating rate of 10 °C/min by using Netzsch STA 409 Simultaneous Thermal Analyzer. Dielectric profiles of the $Bi_4(TiO_4)_3$ ceramic powder were measured in the frequency range of 200 Hz–3 MHz at 300 K on a Hioki 3532-50 LCR meter.

3. Results and discussion

The XRD profile of $Bi_4(TiO_4)_3$ ceramic powder is shown in Fig. 1. The XRD patterns that are indexed in the figure are in good agreement with the orthorhombic structure reported in JCPDS Card No.12-0213. The crystallite size of the prepared ceramic powders has been estimated from the Scherer's equation, $D = 0.9\lambda/\cos\theta$, where D is the crystallite size, λ is the X-ray wavelength (0.15405 nm), θ and β are the diffraction angle and full width at half maximum (FWHM) of an observed peak respectively [12]. Intense diffraction peaks have been selected to compute the crystallite size and it is found to be in an average size of 66 nm.

SEM micrograph of the $Bi_4(TiO_4)_3$ ceramic powder is shown in Fig. 2. The obtained micrograph shows that the particles are agglomerated and irregular in shape. Therefore, the average diameter of the grain size has approximately been measured and it is in the range of 1 μm. The narrow widths of the diffraction peaks also indicate that the prepared ceramic

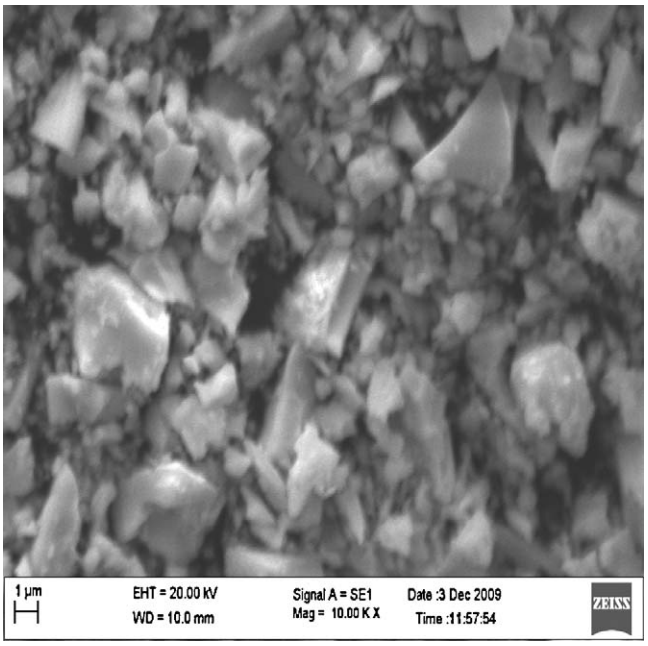

Fig. 2. SEM image of $Bi_4(TiO_4)_3$ ceramic powder.

powders possess large sized grains [13]. It may be mentioned that crystalline powders in micrometer dimension could display high luminescent intensities [14]. EDS spectrum was measured to carry out the elemental analysis of synthesized $Bi_4(TiO_4)_3$ ceramic powder. The obtained elemental characteristic X-ray radiation for Bi of M_α 2.4 keV, L_α 10.8 keV and L_β 13.0 keV, Ti of K_α 4.5 keV and K_{ab} 4.9 keV and oxygen of K_α 0.5 keV respectively [5]. The existence of the unassigned carbon peak at 0.2 keV in the EDS spectrum does not belong to the prepared sample, it is due to the carbon tape that was used to hold the specimen during the measurement (Fig. 3).

The FTIR spectrum of the $Bi_4(TiO_4)_3$ ceramic powder was recorded at the room temperature and is shown in Fig. 4. Three sharp bands at 815 cm^{-1}, 580 cm^{-1} and 400 cm^{-1} are observed. The former two bands are ascribed to the Ti–O

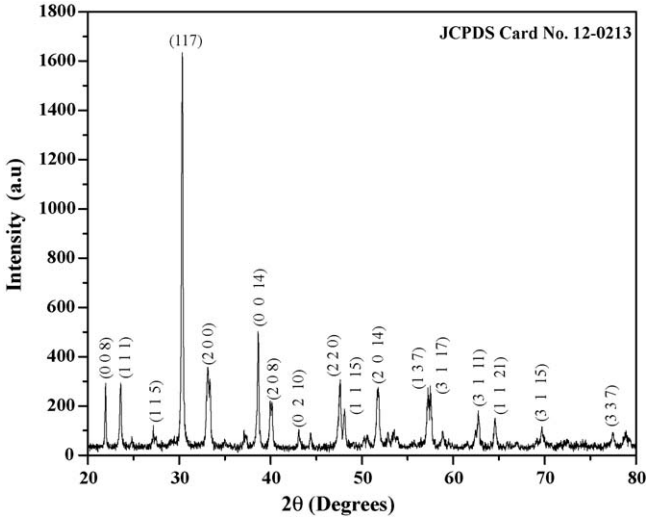

Fig. 1. XRD profile of $Bi_4(TiO_4)_3$ ceramic powder.

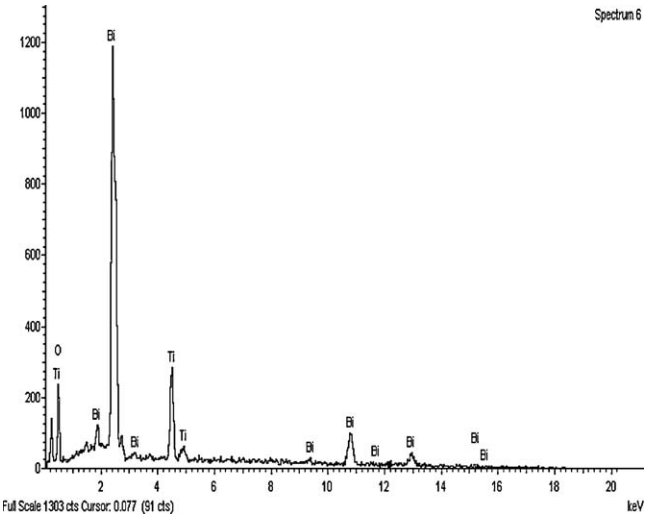

Fig. 3. EDS profile of $Bi_4(TiO_4)_3$ ceramic powder.

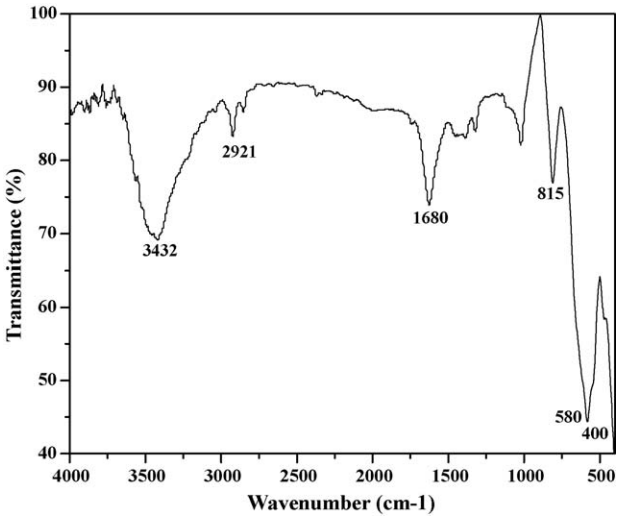

Fig. 4. FTIR spectrum of $Bi_4(TiO_4)_3$ ceramic powder.

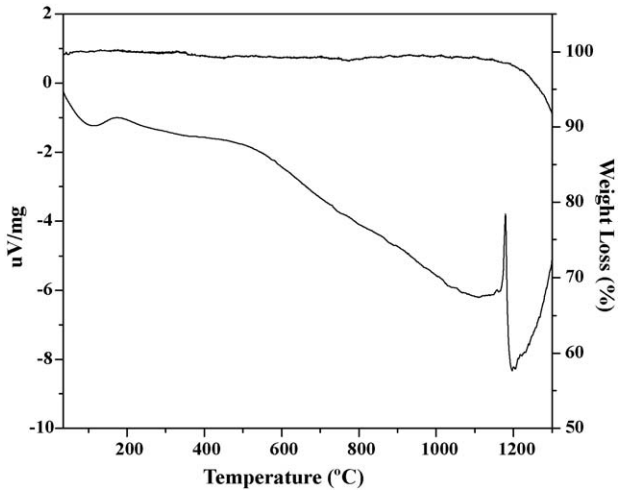

Fig. 6. TG–DTA curves of $Bi_4(TiO_4)_3$ ceramic powder.

stretching vibrations, while the latter one to the Ti–O bending vibrations [15]. Due to the absence of a C=O vibration at around 1450 cm^{-1}, it follows that the powder is free from carbonates. This result is satisfactory from a technological point of view since most of the properties are dependent on the quality of the raw powder used [16]. Bands at 2921 cm^{-1} and 3432 cm^{-1} arise from the antisymmetric and symmetric stretching band of H_2O and OH groups, while a band at 1680 cm^{-1} corresponds to the bending vibrations of H_2O. These three bands are the characteristic vibrations of moisture presence in the sample surface [17].

Fig. 5 shows the Raman spectrum of $Bi_4(TiO_4)_3$ ceramic powder. Stronger Raman peaks imply the strong interactions between the atoms, which mainly arise from the stretching and bending of the shorter metal–oxygen bonds within the anionic groups. The TiO_6 octahedra in the $Bi_4(TiO_4)_3$ ceramic powder, accordingly, should play an important role in the lattice vibrations. In accordance with Raman data of $Bi_4Ti_3O_{12}$, $BaTiO_3$, and $PbTiO_3$ [18], a shorter bond length of Ti–O compared to Bi–O suggests that the Raman phonon mode at 849 cm^{-1}, originates mainly from the vibrations of atoms inside the TiO_6 octahedra. It is attributed to the symmetric Ti–O stretching vibration. The modes at 540 cm^{-1} (TO) and 565 cm^{-1} (LO) indicate the doubly degenerate symmetric O–Ti–O stretching vibrations. They split into a longitudinal (LO) and transverse (TO) components due to the long-range electrostatic forces that might be associated with lattice ionicity. The 268 cm^{-1} and 227 cm^{-1} modes are ascribed to the O–Ti–O bending vibrations. Although the mode at 227 cm^{-1} is a Raman inactive according to the O_h symmetry of TiO_6, it is often observed because of the distortion of octahedron. The mode at 324 cm^{-1} is due to a combination of the stretching and bending vibrations. Two modes at 538 cm^{-1} and 558 cm^{-1} correspond to the opposing excursions of the external apical oxygen atoms of the TiO_6 octahedra. The TiO_6 octahedra have shown a considerable distortion at the room temperature so that some phonon modes at 324 cm^{-1}, 538 cm^{-1} and 849 cm^{-1} appear wide but weak. The Raman

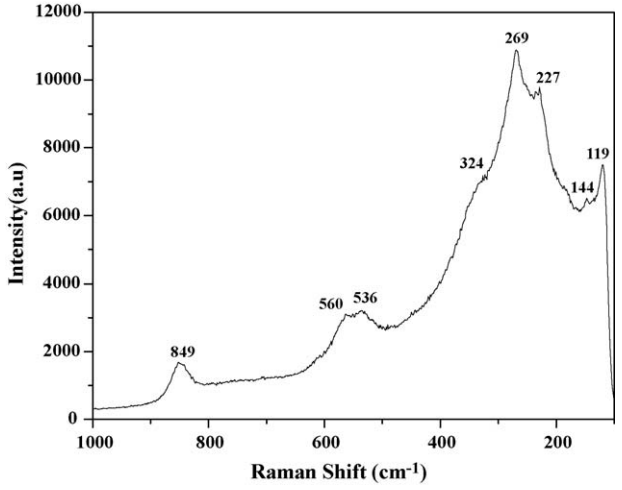

Fig. 5. Raman spectrum of $Bi_4(TiO_4)_3$ ceramic powder.

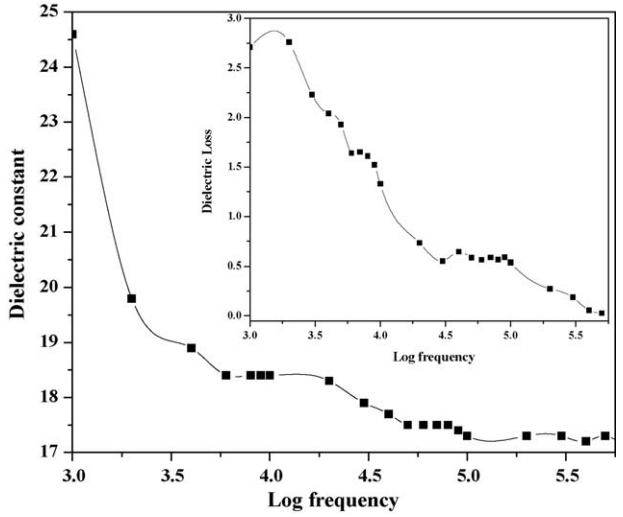

Fig. 7. Variation of dielectric constant (ε') and dielectric loss (ε'') of $Bi_4(TiO_4)_3$ ceramic powder with respect to frequency change at room temperature.

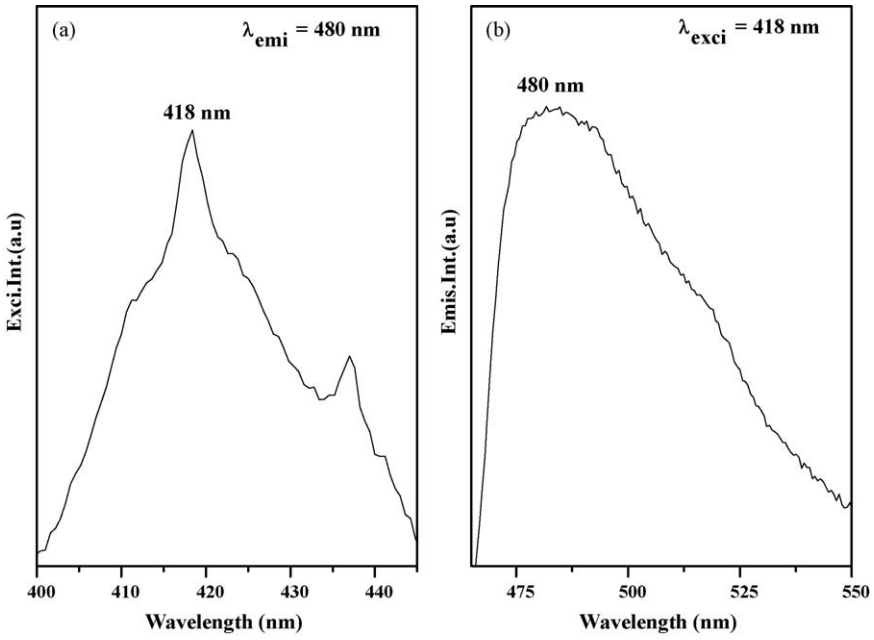

Fig. 8. (a) Excitation and (b) emission spectrum of $Bi_4(TiO_4)_3$ ceramic powder.

modes at 118 cm^{-1} and 144 cm^{-1} originate due to the vibrations between Bi and O atoms. All the assignments have been made based on the literature reports [18–20].

Fig. 6 shows the TG–DTA simultaneous analysis of $Bi_4(TiO_4)_3$ precursor powder which is mixed in a stoichiometric proportions. A sharp exothermic peak at around 1100 °C is attributed to the heat loss during the crystallization of $Bi_4(TiO_4)_3$ ceramic powder. The homogenous mixture of Bi_2O_3 and Ti_2O_3, when it was heated at 1100 °C for 5 h, show an XRD pattern corresponding to $Bi_4(TiO_4)_3$ (JCPDS Card No. 12-0213) which supports the assignment of the exothermic peak at 1100 °C in the DTA curve as due to the crystallization of $Bi_4(TiO_4)_3$. No significant weight loss was found in the TG curve up to 1100 °C temperature and there after the precursor starts decomposing.

Frequency dependence of dielectric constant (ε') and dielectric loss (ε'') of the $Bi_4(TiO_4)_3$ ceramic powder was carried out between 200 Hz and 3 MHz at the room temperature as shown in Fig. 7. The dielectric behavior of the $Bi_4(TiO_4)_3$ ceramics powder is measured in a capacitance cell, consisting of two electrodes of parallel plate in geometry of plate area A and spacing d. The oscillating field is applied to the sample over a wide range of frequency and the capacitance (C) and dielectric loss G/ω, where G is the conductance, as explained here. The real and imaginary parts of susceptibility could be correlated as:

$$C(\omega) = \frac{A^0\varepsilon_0}{d}[\chi'(\omega) + \varepsilon(\alpha)] = \frac{\varepsilon_0\varepsilon_r' A}{d} \quad (1)$$

$$\frac{G(\omega)}{\omega} = \frac{A^0\varepsilon_0}{d}[\chi''(\omega)] = \frac{\varepsilon_0\varepsilon_r'' A}{d} \quad (2)$$

where ε_0 is the permittivity of free space (8.854×10^{-12} F m^{-1}), ε' and ε'' are the real and imaginary parts of the relative permittivity of the sample, respectively [21]. It has been observed that both $\varepsilon'$and ε'' decrease with an increase in frequency which explains the dielectric behavior of the synthesized ceramic powder. This is due to a phenomenon of frequency dispersion. The frequency of hopping between the ions could not follow the frequency of applied field and hence it lags behind, therefore the value of ε' becomes reduced at higher frequencies. The defects, space charge formation, lattice distortions, etc. in the boundaries produce an absorption current resulting in a loss factor (tan δ) and at high alternating frequency those could follow the field applied and at later values the trend appears saturated [22].

Fig. 8(a) shows an excitation spectrum of $Bi_4(TiO_4)_3$ ceramic powder with an emission at λ_{emis} = 480 nm and it has revealed a strong excitation band at 418 nm. Fig. 8(b) shows the emission spectrum of $Bi_4(TiO_4)_3$ ceramic powder in the wavelength range of 450–750 nm with an excitation at 418 nm. We have noticed a strong blue emission at 480 nm ascribed to the electron–hole recombination of localized exciton. Electrons in the valence band are excited to some localized levels and thus form small polarons, and the electron polarons interact with holes possibly trapped near oxygen vacancies to form localized exciton, such as self trapped exciton. The recombination of the localized excitons could be resulting in blue emission as has been reported in the literature [23]. Electron–hole recombination of localized excitons associated with oxygen vacancies could therefore be a possible reason for this blue emission.

4. Conclusion

In brief, blue colour emitting ferroelectric $Bi_4(TiO_4)_3$ ceramic powder has successfully been prepared by a mixed oxide ceramic method. XRD and SEM analysis indicate that this ceramic powder possesses orthorhombic structure and the

particles are approximately in 1 μm in size. FTIR spectrum has revealed the functional groups present in the prepared ceramics. TG–DTA profiles have substantiated that 1100 °C could be the optimum sintering temperature. $Bi_4(TiO_4)_3$ ceramic powder has revealed a strong blue emission at 480 nm and it arises due to electron–hole recombinations of localized excitons that associate with the oxygen vacancies.

Acknowledgements

We would like to thank the Sophisticated Analytical Instrumentation Facility (SAIF) centre, Indian Institute of Technology, Chennai for their kind cooperation and support in our availing their facilities in the measurement of TG–DTA and Luminescence profiles.

References

[1] S. Chatterjee, P.K. Mahapatra, Structural, electrical and dielectric properties of $Na_2W_4O_{13}$ ceramic, Journal of Materials Science Letters 22 (2003) 99–101.

[2] W. Su, J. Lee, Bismuth titanate nano particles dispersed polyacrylates, Journal of Materials Research 19 (8) (2004) 2343–2348.

[3] R.C. Oliveira, L.S. Cavalcante, J.C. Sczancoski, E.C. Aguiar, J.W.M. Espinosa, J.A. Varela, P.S. Pizani, E. Longo, Synthesis and photoluminescence behavior of $Bi_4Ti_3O_{12}$ powder obtained by the complex polymerization method, Journal of Alloys and Compounds 478 (2009) 661–670.

[4] D. Chen, X. Jiao, Hydrothermal synthesis and characterization of $Bi_4Ti_3O_{12}$ powder from different precursors, Materials Research Bulletin 36 (2001) 355–363.

[5] P. Pookmanee, P. Boonphayak, S. Phanichphant, Chemical synthesis of bismuth titanate microparticles, Ceramics International 30 (2004) 1917–1919.

[6] J.S. Bae, J.H. Jeong, K.S. Shim, B.K. Moon, S. Yi, J.H. Kim, Crystallinity and morphology dependent luminescence of Li-doped $Y_{2-x}Gd_xO_3:Eu^{3+}$ thin film phosphors, Applied Surface Science 252 (2006) 4564–4568.

[7] C.C. Yu, X.M. Liu, M. Yu, C.K. Lin, C.X. Li, H. Wang, J. Lin, Enhanced photoluminescence of $Ba_2GdNbO_6:Eu^{3+}/Dy^{3+}$ phosphors by Li^+ doping, Journal of Solid State Chemistry 180 (2007) 3058–3065.

[8] Z. Liu, J. Zhang, B. Han, J. Du, T. Mu, Y. Wang, Z. Sun, Solvothermal synthesis of mesoporous Eu_2O_3–TiO_2 composites, Microporous Mesoporous Materials 81 (2005) 169–174.

[9] R. Pazik, D. Hreniak, W. Strek, A. Speghini, M. Bettinelli, Structural and luminescence properties of Eu^{3+} doped $BaxSr_{1-x}TiO_3$ (BST) nanocrystalline powder prepared by different methods, Optical Materials 28 (2006) 1284–1288.

[10] R. Chen, F. Song, D. Chen, Y. Peng, Improvement of the luminescence properties of $CaTiO_3$:Pr obtained by modified solid-state reaction, Powder Technology 194 (2009) 252–255.

[11] H. Guo, N. Dong, M. Yin, W. Zhang, L. Lou, S. Xia, Green and red upconversion luminescence in Er^{3+}-doped and Er^{3+}/Yb^{3+}-codoped $SrTiO_3$ ultrafine powder, Journal of Alloys and Compounds 415 (2006) 280–283.

[12] S.R. Dhage, Y.B. Khollam, S.B. Dhespande, H.S. Potdar, Synthesis of bismuth titanate by citrate method, Materials Research Bulletin 39 (2004) 1993–1998.

[13] W. Li, D. Su, J. Zhu, Y. Wang, Mechanical and dielectric relaxation in neodymium-modified bismuth titanate ceramics, Solid State Communications 131 (2004) 189–193.

[14] X. Xiao, B. Yan, Chemical co-precipitation synthesis and photoluminescence of Eu^{3+} or Dy^{3+} doped $Zn_3Nb_2O_8$ microcrystalline phosphors from hybrid precursors, Materials Science and Engineering B 136 (2007) 154–158.

[15] N. Pavlovic, D. Kancko, K.M. Szecsenyi, V.V. Srdic, Synthesis and characterization of Ce and La modified bismuth titanate, Processing and Application of Ceramics 3 (1–2) (2009) 88–95.

[16] Z. Simoes, E.C. Aguiar, A. Ries, E. Longo, J.A. Varela, Niobium doped $Bi_4Ti_3O_{12}$ ceramics obtained by the polymeric precursor method, Materials Letters 61 (2007) 588–591.

[17] F. Lei, B. Yan, Hydrothermal synthesis and luminescence of $CaMO_4:RE^{3+}$ (M = W, Mo; RE = Eu, Tb) submicro-phosphors, Journal of Solid State Chemistry 181 (2008) 855–862.

[18] Z.C. Ling, H.R. Xia, W.L. Liu, H. Han, X.Q. Wang, S.Q. Sun, D.G. Ran, L.L. Yu, Lattice vibration of bismuth titanate nanocrystals prepared by metalorganic decomposition, Materials Science and Engineering B 128 (2006) 156–160.

[19] W.L. Liu, H.R. Xia, H. Han, X.Q. Wang, Structural and dielectrical properties of bismuth titanate nanoparticles prepared by metalorganic decomposition method, Journal of Crystal Growth 269 (2004) 499–504.

[20] Z. Hu, H. Gu, Y. Hu, Y. Zou, D. Zhou, Microstructural, Raman and XPS properties of single-crystalline $Bi_{3.15}Nd_{0.85}Ti_3O_{12}$ nanorods, Materials Chemistry and Physics 113 (2009) 42–45.

[21] G. Reshmi, P.M. Kumar, M. Malathi, Preparation, characterization and dielectric studies on carbonyl iron/cellulose acetate hydrogen phthalate core/shell nanoparticles for drug delivery applications, International Journal of Pharmaceutics 365 (2009) 131–135.

[22] S.B. Narang, D. Kaur, S. Bahel, Dielectric properties of lanthanum substituted barium titanate microwave ceramics, Materials Letters 60 (2006) 3179–3182.

[23] H. Gu, Z. Hu, Y. Hu, Y. Yuan, J. You, W. Zou, The structure and photoluminescence of $Bi_4Ti_3O_{12}$ nanoplates synthesized by hydrothermal method, Colloids and Surfaces A: Physicochemical Engineering Aspects 315 (2008) 294–298.